

Synthesis, Characterizations and *in Vitro* Assessment of the Cytotoxicity and Genotoxicity of Novel Silicon Nitride-Based Porous Ceramics

Miroslav Hnatko^{1*}, Zoltán Lenčes¹, Peter Čopan², Lucia Birošová³, Patrik Matejov³, Soňa Jantová³

¹Department of Ceramic, Institute of Inorganic Chemistry, Slovak Academy of Sciences, Bratislava, Slovakia; ²Institute of Inorganic Chemistry, Technology and Materials, Faculty of Chemical and Food Technology, Slovak University of Technology, Bratislava, Slovakia; ³Institute of Biochemistry, Nutrition and Health Protection, Faculty of Chemical and Food Technology, Slovak University of Technology, Bratislava, Slovakia.

Email: *uachmiho@savba.sk

Received April 4th, 2013; revised May 16th, 2013; accepted May 28th, 2013

Copyright © 2013 Miroslav Hnatko *et al.* This is an open access article distributed under the Creative Commons Attribution License, which permits unrestricted use, distribution, and reproduction in any medium, provided the original work is properly cited.

ABSTRACT

Porous Si₃N₄-SiO₂-based ceramics with different porosity were prepared via free sintering of Si₃N₄ on air with an addition of semolina (5, 10 and 20 wt%) as a pore-forming agent. The semolina content in the starting powder controlled the volume fraction of pores in the sintered body. Small pores (<5 μm) formed a continuous network in the whole volume of the ceramic material, while the large pores (~100 μm), formed from the added semolina were mostly isolated in the ceramic matrix. Mercury porosimetry and strength measurements have shown that specific surface area, volume density and compressive strength decreased with the amount of semolina in the samples. Mechanical properties similar to bone were obtained for the sample with 20 wt% semolina pore forming agent (compressive strength 350 MPa, density 2.17 g·cm⁻³). The prepared Si₃N₄-SiO₂-based ceramics were evaluated for cytotoxic and genotoxic potential on human fibroblast VH10 and B-HNF-1 cells. Biological tests have shown that both these human fibroblast cell lines were sensitive to the samples with lower porosity and cell growth inhibition was observed in the range 14.9% - 21.3%. The cytotoxicity of the sample with the highest porosity (~40%) was not significant (<10%). The microscopic observations have shown that VH10 and B-HNF-1 cells growing around the silicon nitride ceramic discs were homogeneously distributed on the cultivation surface. No significant morphologic changes were found in treated cells, their morphology was very similar to that of the control cells. None of the tested Si₃N₄-based ceramic samples induced necrotic/apoptotic death of human fibroblasts. Sample S-20 had similar properties to bones and was characterized by very good biocompatibility, slight cytotoxicity and none genotoxicity. Therefore, Si₃N₄-SiO₂-based ceramics prepared by free sintering on air are potential biomaterials for medical applications.

Keywords: Silicon Nitride; Sintering; Porosity; Mechanical Properties; Cytotoxicity/Genotoxicity; Human Cell Lines

1. Introduction

Silicon nitride ceramics belong to the well-established engineering materials and are used for applications where their favorable mechanical, tribological, thermal and chemical properties can be utilized. Except of high performance industrial applications of Si₃N₄-based ceramics the scientific community has focused attention in the last decade on the perspectives and potentials of these ceramics for bio-applications [1]. These materials have a potential use as biomaterials, permanent clinical devices, and articular prosthesis or for reconstructive bone sur-

gery as fixture systems. Recent results confirmed the non-cytotoxicity of these materials and the *in vivo* tests of Si₃N₄ pieces implanted into femurs of rabbits showed good bone/implant attachment with no immuno-inflammatory or adverse cell reactions [2]. Multiple studies have evaluated the biological responses of cell culture and animal models to Si₃N₄ and confirmed their biocompatibility [3-5]. Some biological tests suggested that Si₃N₄-based ceramics have comparable or even better Osseo-integration than alumina [4,6]. It was also reported that in cells growth on polished silicon nitride surface, the parameters concerning viability and morphology are comparable to those of titanium [7]. Porous intramedul-

*Corresponding author.

lary Si_3N_4 rods implanted in rabbit supported the bone growth. Moreover, detailed investigations on the influence of different qualities of commercial silicon nitride-based materials revealed no correlations between cell yields and chemical composition [8]. The *in vitro* biocompatibility tests of polished sintered reaction bonded silicon nitride (SRBSN) showed that this ceramic material promotes the proliferation of human osteoblast-like MG-63 cells [9,10]. The test of Si_3N_4 implants in rabbits also showed promising results including biocompatibility, osteoconduction and bone remodeling adjacent to the ceramic implant surfaces [11-13].

Owing to the above mentioned properties Si_3N_4 -based ceramics have already been considered as biomaterials, in particular for orthopaedic and dental applications [14, 15] or for biosensors [16], microelectro-mechanical systems (MEMS) of medical devices [17,18], and membranes for blood-brain barrier [19].

The mechanical properties of silicon nitride-based ceramics are strongly dependent on their microstructure. In certain level of porosity the silicon nitride offers an interesting combination of strength and stiffness [20]. Porous Si_3N_4 -based ceramics with high porosity is a promising candidate for engineering applications, such as hot gas filter, heat insulators, catalyst carriers, bioreactors, medical implants, etc. [21,22]. For industrial applications several kinds of porous Si_3N_4 -based ceramics with different mechanical, thermal and chemical properties were prepared by different fabrication routes [20,23-28]. Chen *et al.* used pressure-less sintering technique and phosphoric acid (H_3PO_4) as the pore-forming agent for the preparation of relatively high strength (50 - 120 MPa) porous Si_3N_4 ceramics [29]. Other authors prepared porous Si_3N_4 ceramics with high porosity (48% - 60%) and flexural strength of 100 - 145 MPa via nitridation of Si powder compact [8].

The application of either dense, or porous Si_3N_4 ceramics in human body requires a standardized biological safety—biocompatibility tests (ISO 10993-1). Biocompatibility is the ability of a material to perform with an appropriate host response in a specific application. Cytotoxicity and genotoxicity testing represents the initial phase in testing biocompatibility of potential biomaterials and medical devices. Cytotoxicity testing includes numerous qualitative and quantitative methods that use different cells growing *in vitro* for biomaterial testing. Many compounds show cytotoxic effect by the induction of cell death, which can be divided into three classes, apoptosis, necrosis and autophagy. Apoptosis has been described as multiple pathways converging from numerous different initiating events and insults. Morphological changes of apoptosis are considered as results of complex cellular biochemical pathways. Necrosis is the end

result of a bioenergetics catastrophe resulting from adenosine triphosphate (ATP) depletion to a level incompatible with cell survival and was thought to be initiated mainly by cellular “accidents”, such as toxic insults or physical damage. Generally is known that apoptosis/necrosis can be evoked by deoxyribonucleic acid (DNA) damage.

In this study porous Si_3N_4 - SiO_2 -based ceramic discs with various porosities were prepared by pressure-less sintering of Si_3N_4 on air with an addition of semolina as pore forming agent. Further, the microstructure, mechanical properties, biocompatibility, cytotoxicity and genotoxicity of porous Si_3N_4 - SiO_2 -based ceramics were investigated. Human fibroblast cell lines VH10 and B-HNF-1 were used for biological tests. The cytotoxicity was determined by the direct contact test—vital staining, direct counting of adherent and growing cells and the assessment of release of lactate dehydrogenase (LDH). Comet assay was used for genotoxic study.

2. Materials and Methods

2.1. Preparation of Porous Si_3N_4 - SiO_2 -Based Ceramics and Their Characterization

For the preparation of porous ceramics α - Si_3N_4 powder ($\alpha > 94\%$, O < 1.5%, N > 38.5%, Si (free) < 0.15%, C < 0.1%, Fe < 120 ppm, $d_{50} = 2.4 \mu\text{m}$; produced by Yantai Tomley Hi-Tech Ind. & Tra. Co., Ltd.) and durum wheat semolina (density: $1.4 \text{ g}\cdot\text{cm}^{-3}$, grain size max. 350 μm ; SLAVUS s.r.o. Bratislava, Slovakia) were used. The starting powder compositions are listed in **Table 1**. Semolina and Si_3N_4 were homogenized in different weight ratios in plastic container for 24 h in isopropanol with Si_3N_4 balls. The mixtures were dried in rotary evaporator. After drying, polyvinyl alcohol was added to the mixture (1.3 ml PVA/10 g mixture) to increase the coherence of Si_3N_4 particles and semolina. The powders were first uniaxially pressed into pellets (12 mm \times 5 mm) under 100 MPa and then isostatically pressed under 250 MPa. The annealing conditions for semolina removal from the samples were optimized on the base of simultaneous differential thermal analysis and thermo-gravimetric (DTA/TG) measurements (Simultaneous DTA-TG apparatus, SDT 2960, T. A. Instruments) in the temperature range from 25°C to 600°C. Based on obtained results were samples

Table 1. Composition of samples and their marking.

Sample	Si_3N_4 (wt%)	Semolina (wt%)	Semolina (vol%)
S-5	95	5	10.7
S-10	90	10	20.3
S-20	80	20	36.4

dried at 250°C for 5 h and then fired at 600°C for 5 h in air. The heating/cooling rate was 10°C/min. After burn-out of semolina were samples sintered in air at 1360°C for 3 h. The microstructure of porous samples was analyzed by scanning electron microscope (SEM; EVO® 40 Series, Carl Zeiss AG, Germany) equipped with electron dispersive X-ray analysis.

The crystalline phase composition was identified by X-ray diffraction analysis (XRD; CoK_α radiation, STOE, Germany), and the possible chemical bonds by Fourier transform infrared spectroscopy (FTIR) using Nicolet Magna 750 spectrometer.

The values of specific surface area, density and volume density of porous ceramics were measured by mercury porosimetry (Porosimeter P2000, Fisons Instruments, USA) using the model of the cylindrical shape of pores. The compressive strength of Si₃N₄-SiO₂-based ceramic samples was measured with an indentor (diameter: 2.025 mm) from quenched steel on TIRAFEST 2300 (Lloyd) tester with a cross-head speed of 0.5 mm/min. The tested samples (10 of each series) had a cylindrical shape (diameter 12 mm, height 5 - 8 mm) and both sides of samples were grinded on diamond disc (diamond grains size: 20 μm) before measurement.

For biological experiments the Si₃N₄-SiO₂-based ceramic discs were sterilized at 130°C for 30 min.

2.2. Biocompatibility Tests

2.2.1. Materials

The following materials were used for biocompatibility tests: Dulbecco's modified Eagle medium (DMEM), fetal bovine serum (FBS), trypsin and antibiotics were purchased from Biocom Co. (Bratislava, Slovakia); Trypan blue, ethidium bromide (EtBr), low melting-point agarose (LMP), normal melting point agarose (NMP), Triton-X-100 (9002-93-1), Na₂EDTA, Tris-HCl, pyruvate sodium salt and reduced nicotinamide adenine dinucleotide (NADH) were obtained from Sigma Chemical Co. (St. Louis, MO, USA); proteinase K and RNA-ase were purchased from Serva (Germany).

2.2.2. Cell Culture

Human fibroblast cell lines VH10 and B-HNF-1 cells were obtained from the American Type Culture Collection (Rockville, MD, USA). The cells (starting inoculum 1.0 × 10⁵ VH10 cells/mL and 5 × 10⁴ B-HNF-1 cells/mL) were grown in completely Dulbecco's modified Eagle medium (DMEM) supplemented with 10 vol% fetal bovine serum, penicillin G (100 mg/L), streptomycin (100 mg/L) and kanamycine (100 mg/L) at 37°C in humidified 6% CO₂ and 94% air atmosphere. Before a confluent monolayer was formed, the cells were harvested from the culture surface by incubation with a 0.25% solution of

trypsin. When a suitable cell concentration was reached, the suspension was used for the experiments. The cells were just in the exponential phase of growth. All experiments were performed in Petri dishes (Ø 60 mm). Cell viability was determined by a trypan blue exclusion test.

2.2.3. Direct Contact Cytotoxicity Test

The basal cytotoxicity of silicon nitride-based discs with different porosity (S-5, S-10, S-20) was determined using the method of direct cell counting [30]. First the tested ceramic discs (diameter 10 mm) were placed in the centre of the Petri dishes, under sterile condition. Then VH10 and B-HNF-1 cells were re-suspended in culture medium at density of 5 × 10⁵ VH10 cells/mL and 2.5 × 10⁵ B-HNF-1 cells/mL and plated into 60 mm Petri dishes in a total volume of 5 mL medium. The dishes were incubated at 37°C for 96 h in a humidified atmosphere of 6% CO₂ in air. The negative control (NC) was performed by seeding cell suspension in the Petri dishes without the tested Si₃N₄ samples in the centre. Cell proliferation was evaluated after 96 h in the absence or with the presence of silicon nitride-based discs. After 96 h, the medium was removed and adherent fibroblast cells from three samples of each Si₃N₄-SiO₂ disc were enzymatically released with trypsin (0.25%) for 3 min at 37°C and counted in a Bürker chamber. Treated and control cells viability was determined by 0.4% trypan blue staining.

Cytotoxic effect of silicon nitride-based discs was evaluated in terms of inhibition of cell proliferation. Relative cell growth was calculated using the following equation:

$$\% \text{ of viable cells} = (K - E) / (K - K_0) * 100 \quad (1)$$

where K_0 is the cell number at the time of the addition of biomaterial, K is the cell number after 96 h of cultivation without the Si₃N₄-SiO₂ discs and E is the cell number after 96 h of cultivation with the biomaterial.

The cellular morphology was observed with a light microscope (Meopta, Slovakia).

2.2.4. LDH Quantification

Measurement of lactate dehydrogenase (LDH) release is an important and frequently applied test for cellular membrane permeabilization and severe irreversible cell damage. The amount of released LDH was measured according to Bergmeier [31].

After incubation periods, the medium was aspirated from each sample together with the control and stored on ice. Then, the standard solutions for samples with released LDH was prepared (containing 100 mM Tris-HCl buffer, pH = 7.1, 15 mM of NADH and 1.0 M of pyruvate sodium salt) as well as the standard solution of the total LDH (the same composition but plus 10% solution of Triton-X-100). The standard solutions were incubated

at 31°C for 5 - 10 min before the measurement. Oxidation of NADH was measured by the photometer MULTISKAN® FC (Thermo Scientific, USA) at 340 nm. The absorbance decreased linearly with time over 60 s of measurement [32].

2.2.5. Agarose Gel Electrophoresis

The control and VH10 and B-HNF-1 cells treated with silicon nitride-based discs for 96 h were harvested, washed in PBS and lysed in 100 µL of solution containing 10 mM of Tris-HCl, 10 mM of EDTA and 0.5 wt% of Triton X-100 supplemented with proteinase K (1 mg/mL). Samples were then incubated at 37°C for 1 h and heated at 70°C for 10 min. A repeated incubation at 37°C for 1 h followed after adding RNA-ase (200 µg/mL). The samples were subjected to electrophoresis at 40 V for 3 h in 2 wt% agarose gel complemented with ethidium bromide (EtBr; 1 µg/mL). Separated DNA fragments were visualized using the UV transilluminator (254 nm, UltraLum Electronic UV Transilluminator, USA).

2.2.6. Comet Assay

The Single Cell Gel Electrophoresis (SCGE) assay, better known as the comet assay, is a sensitive technique detecting single and double strand breaks and/or alkali-labile sites at the single cell level on DNA of any kind of cells [33]. We used the comet assay to detect induction of DNA damage in VH10 and B-HNF-1 cells after 96 h growth with/without the presence of Si₃N₄-SiO₂ samples. The procedure of Singh *et al.* [34] was used with minor changes suggested by Slameňová *et al.* [35] and Gábelová *et al.* [36]. A base layer of NMP agarose (100 µL of 0.75 wt%) in PBS buffer (Ca²⁺ and Mg²⁺ free) was placed on microscope slides. Human fibroblast VH10 and B-HNF-1 cells were grown with/without the Si₃N₄-SiO₂ samples for 96 h. Both treated and control cells were suspended in LMP agarose (0.75 wt%). The aliquot of 85 µL of LMP agarose, containing 2 × 10⁴ cells, was spread on the base layer. Triplicate slides were prepared per sample. After solidifying of agarose, the slides were placed into the lyses mixture (composed of 2.5 M NaCl, 100 mM Na₂EDTA, 10 mM Tris-HCl, pH = 10.0 and freshly added 1% Triton X-100) at 4°C. The slides were then transferred to the electrophoresis box with alkaline solution (300 mM NaOH, 1 mM Na₂EDTA, pH > 13) and kept in this solution for 40 min at 4°C to unwind DNA strands. The voltage 25 V and current 300 mA were applied for 30 min. The slides were removed, neutralized by 2 × 10 min washing in tris-HCl (0.4 M, pH = 7.5) and stained with 20 µL EtBr (10 µg/mL of EtBr). Stained nucleoids were evaluated with the Zeiss Jenalumar fluorescence microscope (magnification 200×). For each sample 100 comets were scored by the computer-

ized image analysis (Komet 5.5 Europe, Kineting Imaging, Liverpool, UK) to determine DNA in the tail, linearly related to the frequency of DNA strand breaks [33, 37].

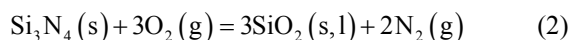
2.2.7. Statistical Analysis

All the cell experiments were performed in triplicate with at least three replications. Statistical analysis was performed with the ANOVA (analysis of variance) test for nonparametric measurements. The significance of differences between values acquired by comet assay was evaluated by student's *t*-test statistically different from the control. All biological tests were conducted at the *p* < 0.05 significance level.

3. Results and Discussion

3.1. Porous Si₃N₄-Based Ceramic Body

The preliminary sintering experiments showed that Si₃N₄-based ceramics are easily oxidized in air at temperatures above 900°C. The surface of Si₃N₄ ceramics is changed to SiO₂ by passive oxidation according to the following reaction [25]:



The oxidized surface was analyzed by SEM-EDX, XRD and FTIR on the sample S-20 with the highest initial semolina content (20%). The results obtained from the EDX analysis for pure Si₃N₄ starting powder and sintered sample S-20 are shown in **Figure 1**. The ratio N:O significantly changed from 8 for Si₃N₄ powder to 0.27 for the oxidized sample. This observation suggests a strong oxidation of Si₃N₄ under the used sintering conditions. FTIR spectroscopy detected the Si-O bond (1097 cm⁻¹) as well as Si-N and Si-C bonds. Carbon could originate from the non-perfect burn out of semolina at 600°C in air and during sintering at higher temperatures SiC was formed [38].

The phase composition of samples sintered at 1360°C in air for 1, 2 and 3 h was determined by XRD analysis. The results are summarized in **Figure 2** and show that the intensity of SiO₂ diffraction increases with increasing holding time. The evaluation of diffraction patterns by TOPAS profile and structure analysis software give the following contents of crystalline SiO₂ in the samples: 25 wt% (1 h), 34 wt% (2 h) and 38% (3 h). The full width at half maximum (FWHM) of SiO₂ diffraction is larger compared to Si₃N₄ diffractions which suggests small/nano particle size of silica. A broader hump at 2θ = 22° - 27° is characteristic for amorphous silica, or SiOC glasses [39]. Sorarù *et al.* reported that the oxidation of α-Si₃N₄ powder begins at 910°C and up to 1200°C amorphous silica was the only oxidation product [39]. These authors

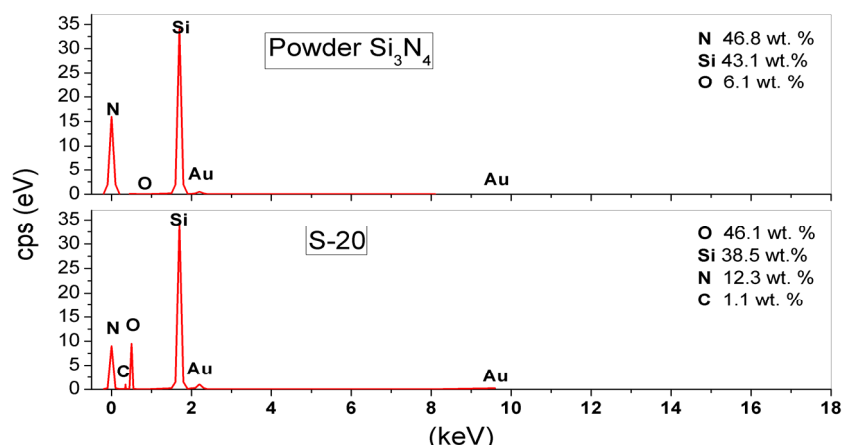


Figure 1. EDX analysis of Si_3N_4 starting powder and sintered S-20 sample (20 wt% semolina content in starting powder).

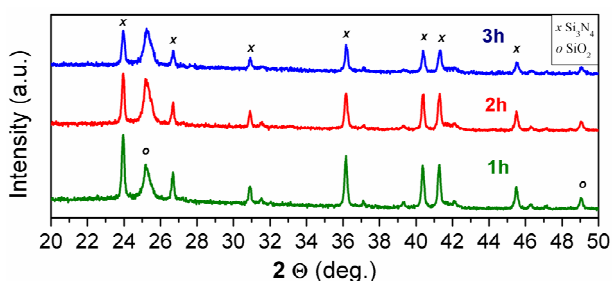


Figure 2. XRD phase analysis of S-20 samples sintered at 1360°C on air (x—diffractions of Si_3N_4).

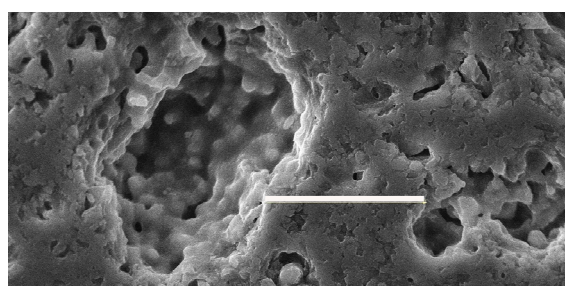
observed weak diffractions of cristobalite at 1300°C which indicates its nucleation and crystallization. At 1400°C , the cristobalite diffractions became more intensive and extensive crystallization of amorphous silica occurred.

Our samples were sintered at 1360°C and for that reason some remaining amorphous silica can be presented in the product, especially in the sample sintered only for 1h. The amorphous silicon oxide-based glass may exhibit bioactivity different from silicon nitride crystalline phase, close/similar to that of silica-rich (45 wt%) bioactive glass [40,41].

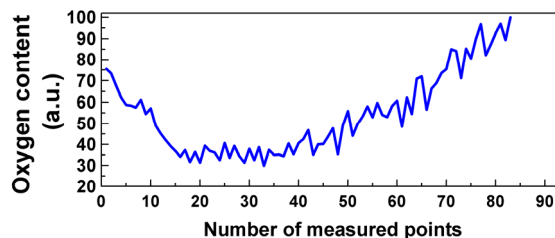
The form of silica (amorphous or cristobalite) has a strong influence on the compactness of the silica layer on Si_3N_4 substrate. Although the coefficient of thermal expansion (CTE) of amorphous silica ($0.5 \times 10^{-6} \text{ K}^{-1}$ at 293 - 1273 K) is smaller than that of Si_3N_4 ($3.0 - 3.3 \times 10^{-6} \text{ K}^{-1}$ at 273 - 1273 K) and can induce some residual stresses during cooling, the CTE of cristobalite is much larger ($14.5 \times 10^{-6} \text{ K}^{-1}$ at 297 - 967 K). Due to the large difference between the CTE of Si_3N_4 and cristobalite remarkable residual stresses are formed during cooling from the sintering temperature and results in microcracking. These cracks deteriorate the mechanical properties of the porous ceramics [29]. On the other hand, it is known that silica increases the efficiency of apatite layer

formation on the sample surface what is an important factor for tissue attachment to the implant [42-44]. For that reason the presence of either amorphous silica or thin amorphous layer containing cristobalite particles on our Si_3N_4 -based ceramic material can be beneficial for bio-applications. However, the thickness of layer containing cristobalite particles should not exceed the critical value ($<15 \mu\text{m}$), when cracks are formed due to the residual stresses. The closer look on the oxidized surface of large pore shows (Figure 3(a)) that the surface layer is free of cracks. The linescan EDX analysis shows an increasing trend of oxygen content towards the large pores (Figure 3(b)).

The structure of Si_3N_4 - SiO_2 -based ceramics was ex-



(a)



(b)

Figure 3. Linescan EDX analysis of oxygen content between two pores in sample S-10.

amed by SEM and the results are shown in **Figure 4**. **Figure 4(a)** shows the distribution of macro-pores. The size of macro-pores in all the resulting materials is around 100 μm and they are isolated. Their volume content is in accordance with the amount of semolina added to the starting powders. The distribution of micro-pores is shown at higher magnification on the fracture surface of samples in **Figure 4(b)**. Obviously, in contrast to the macro-pores, the micro-pores are interconnected irrespective of the macro-pores content.

The results of mercury porosimetry are summarized in **Figure 5** and show that the specific surface area and volume density decreased with the amount of semolina. Therefore, decreasing values are related to the increasing volume fraction of pores in the ceramic materials. **Figure 5** also shows that the densities of the prepared samples did not differ markedly (S-5: 2.45 $\text{g}\cdot\text{cm}^{-3}$; S-10: 2.49 $\text{g}\cdot\text{cm}^{-3}$). The density of the sample S-20 was the lowest (2.17 $\text{g}\cdot\text{cm}^{-3}$), as expected, but within the interval of the density of human cortical bone (1.8 $\text{g}\cdot\text{cm}^{-3}$ - 2.2 $\text{g}\cdot\text{cm}^{-3}$). If we compare the density values of prepared samples with densities of the pure Si_3N_4 (3.20 $\text{g}\cdot\text{cm}^{-3}$) and pure SiO_2 (2.16 $\text{g}\cdot\text{cm}^{-3}$) their densities are closer to that for SiO_2 . This can be a result of better access of oxygen to the whole porous Si_3N_4 sample during sintering on air and formation of silica. Taking into account the determined oxygen content by EDX analysis (**Figure 2**), more than 85 wt% of Si_3N_4 was oxidized in the analyzed surface layer. The effect of the semolina content on the

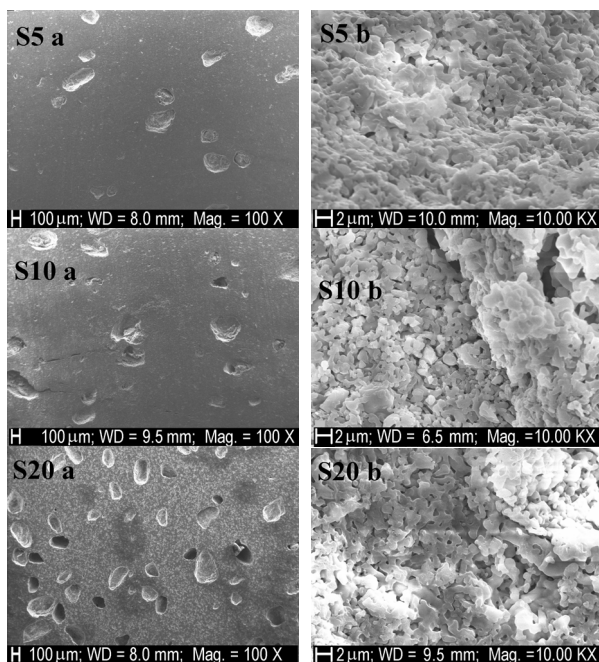


Figure 4. SEM micrographs of porous $\text{Si}_3\text{N}_4\text{-SiO}_2$ -based ceramic samples. (a) Distribution of large pores; (b) Distribution of small pores.

compressive strength of $\text{Si}_3\text{N}_4\text{-SiO}_2$ samples is shown in **Figure 6**.

The total deformation and force during breakage was measured. Final compressive strength was calculated according to the following equation:

$$\sigma_f = 4 \cdot F_f / (\pi \cdot d^2) \quad (3)$$

where F_f is total force during breakage and $d = 2.025$ mm. Deformation during breakage was calculated from the equation:

$$\varepsilon_f = \Delta l / l_0 \quad (4)$$

where l_0 is the starting height of sample and Δl is the change/decrease of height during the test.

The interval of the measured values of compressive strength is large and was probably caused by horizontal and vertical (micro) cracks. It indicates that the addition of semolina affects the compressive strength: higher the volume fraction of semolina in green bodies, lower the compressive strength. Some of the S-20 samples were also isostatically pressed for better handling of green bodies. The isostatic pressing had positive influence on the compressive strength of sintered bodies. If we compare the compressive strength of our porous samples with that of the human bones (up to 360 MPa) it can be concluded that using pressure-less sintering of Si_3N_4 on air we are able to prepare materials with nearly the same compressive strength as a human bone tissue. The mechanical

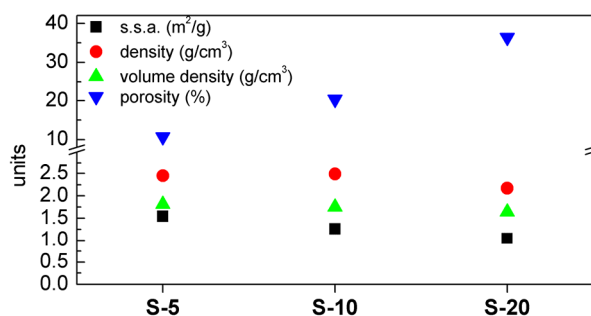


Figure 5. Results of mercury porosimetry on the prepared porous samples. Porosity means the large pores content and it was calculated from the volume content of semolina in $\text{Si}_3\text{N}_4\text{-SiO}_2$ ceramic samples assuming that semolina was completely burned out.

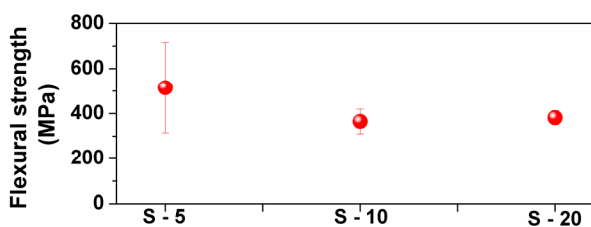


Figure 6. Compressive strength of porous $\text{Si}_3\text{N}_4\text{-SiO}_2$ ceramic samples.

properties and chemical composition of the prepared $\text{Si}_3\text{N}_4\text{-SiO}_2$ composite samples indicate their possible utilization as biomaterials for regenerative medicine. Therefore the cytotoxic and genotoxic potentials of these porous ceramic materials were investigated.

3.2. Biocompatibility Tests

In the biological experiments human fibroblast cell lines VH10 and B-HNF-1 were used as cell model. Cytotoxicity was measured by direct contact assay; genotoxicity was determined by comet assay. The initial steps of *in vitro* cytotoxicity test for $\text{Si}_3\text{N}_4\text{-SiO}_2$ discs included the analysis of cell morphology, cell growth and death of cells growing with the ceramic samples.

First the cell proliferation and morphology was evaluated after 96 h incubation of VH10 and B-HNF-1 fibroblast cells in the presence of $\text{Si}_3\text{N}_4\text{-SiO}_2$ samples with different porosity. The cells grown without the presence of ceramic discs were used as a negative control (NC). The results are shown in **Figures 7 and 8**. As it is shown in **Figure 8**, both fibroblast type human cells have grown

well with $\text{Si}_3\text{N}_4\text{-SiO}_2$ samples, and only slight inhibition of cell proliferation was observed. The cytotoxicity of $\text{Si}_3\text{N}_4\text{-SiO}_2$ samples was in the range from 6.2% to 21.3%. The sensitivity of VH10 and B-HNF-1 cells to the ceramic $\text{Si}_3\text{N}_4\text{-SiO}_2$ discs was on the same level. On the other hand, the porosity of silicon nitride-based samples had an influence on cytotoxicity. The highest cytotoxic effect induced the silicon nitride-based sample S-5 (21.3% for VH10 cells, 20.3% for B-HNF-1 cells), and it was lower for sample S-10 (16.8% for VH10 cells and 14.9% for B-HNF-1 cells). The cytotoxicity of sample S-20 was not significant, the cell growth inhibition was less than 10% (9.7% for VH10 cells and 6.2% for B-HNF-1 cells), **Figure 8**.

The morphology of cells growing with negative control and with porous $\text{Si}_3\text{N}_4\text{-SiO}_2$ samples is shown in **Figure 8**. VH10 and B-HNF-1 cells were placed on the standard Petri dishes and after 24 h incubation the porous $\text{Si}_3\text{N}_4\text{-SiO}_2$ samples were added. The fibroblast cells treated with negative control and $\text{Si}_3\text{N}_4\text{-SiO}_2$ samples were homogeneously distributed on the surface of Petri

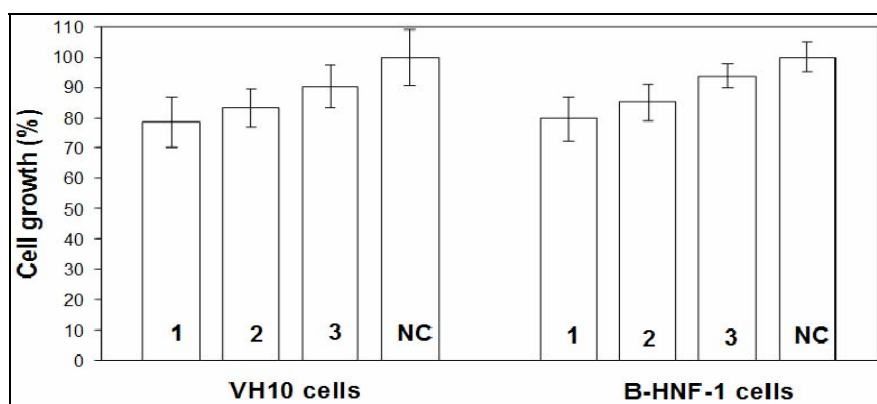


Figure 7. Growth of VH10 and B-HNF-1 cells treated for 96 h with $\text{Si}_3\text{N}_4\text{-SiO}_2$ ceramic samples S-5 (1), S-10 (2) and S-20 (3). The cells growing without the presence of $\text{Si}_3\text{N}_4\text{-SiO}_2$ -based ceramics were used as the negative control (NC).

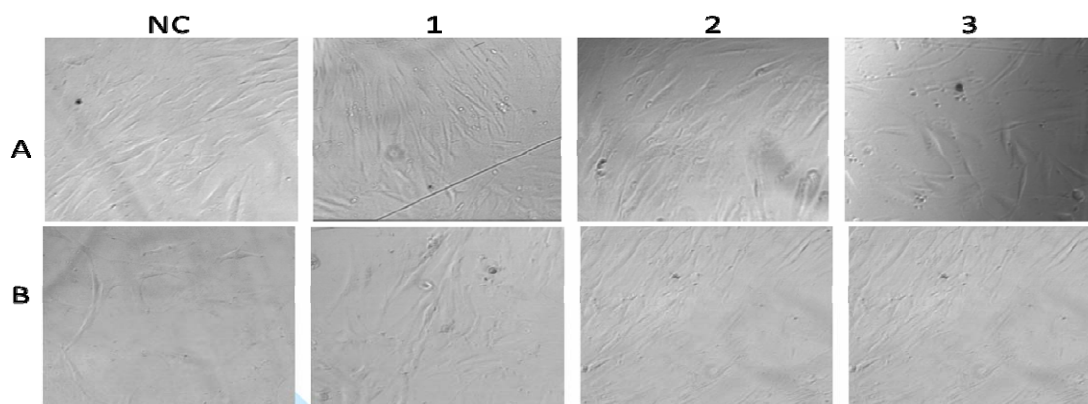


Figure 8. Morphology of VH10 (A) and B-HNF-1(B) cells growing in the presence of silicon nitride samples S-5 (1), S-10 (2) and S-20 (3). The cells growing without the presence of $\text{Si}_3\text{N}_4\text{-SiO}_2$ -based ceramics were used as the negative control (NC). Magnification 250 \times .

dishes and produced a complete monolayer after 96 h of culture. The great majority of them was scattered and exhibited typical fibroblast morphology, an elongated and polygonal shape. In some areas, cells in mitosis were observed. The cells grown in a direct contact with Si₃N₄-based ceramic samples (**Figure 8**) did not show any morphological damage after 96 h of culture. Their morphology was completely similar to that of negative control cells.

The effects of various Si₃N₄ types on cell viability and growth in *in-vitro* conditions were evaluated by some researchers [1,8,45-48]. These materials were mainly biocompatible and non-toxic, their biological properties were dependent on the surface and pore size of biomaterial. On the other hand, Svensson *et al.* [49] investigated the toxicity of Si₃N₄ whiskers and equiaxed powder on V79 cells. Concentration-dependent inhibition of the cloning efficiency of V79 cells was observed with the EC50 (effective concentration of Si₃N₄ samples resulting in 50% of the cell growth that was recorded in control experiments) values 0.9 µg/cm² for Si₃N₄ whiskers and 10.3 µg/cm² for Si₃N₄ powder. The authors assumed that the reason for the measured cytotoxicity could be that these whiskers are very efficient in rupturing the cell membrane. Low cell growth and cytotoxic activity of some Si₃N₄ fibers and nanoparticles were also reported [9,32, 50].

In our samples the remaining Si₃N₄ grains are more equiaxed and 0.7 - 2.5 µm in diameter (**Figures 3(a)** and **4(b)**), so neither the needle-like (whisker) shape, nor the nano-size induced toxicity should show up in the biocompatibility tests.

Based on the obtained results we can conclude that while the porosity of Si₃N₄-SiO₂ samples did not affect the cell morphology, the cytotoxic effect of these silicon nitride-based ceramic samples was porosity dependent. Whereas the samples S-5 and S-10 with lower porosity (10.7 vol% and 20.3 vol%) demonstrated cytotoxicity in the range from 14.9% to 21.3%, the ceramic sample S-20 with the highest porosity (36.4 vol%) had negligible cytotoxicity (<10%). These observations are in agreement with the results of Dongxu *et al.* that Si₃N₄ ceramics with high porosity are promising candidates for bio-applications [21].

In the next experiments we have elucidated the mechanism of cytotoxic activities of Si₃N₄-SiO₂ samples. To analyze the pathway of cell death, we have examined the ability of silicon nitride-based samples to induce necrotic/apoptotic cell death using determination of LDH (lactate dehydrogenase) release from the cells with integrity damage of the cytoplasmic membrane and agarose gel electrophoresis to assess apoptotic DNA fragmentation. The effects of Si₃N₄-SiO₂ samples with various porosity

on the level of LDH release from VH10 and B-HNF-1 cells after 96 h treatment are shown in **Figure 9**. The percentage of LDH release was determined as the ratio of released LDH to the total LDH content. **Figure 9** shows that there was no significant change in the LDH release (<3%) in comparison to the negative control.

Before discussing the results of DNA change during necrotic and apoptotic death, it should be mentioned that the degradation of DNA during necrosis usually occurs randomly, forming a “smear” pattern on agarose gels, while apoptotic DNA fragmentation occurs to oligonucleosome fragments forming a remarkable “ladder” pattern on the gels. In our experiments the apoptotic DNA fragments in VH10 and B-HNF-1 cells treated for 96 h with negative control and Si₃N₄-SiO₂ samples were not observed. On the other hand, positive control (6 µmol·L⁻¹ cisplatin) induced formation of DNA ladder (data are not shown).

On the base of obtained data we can conclude that the studied porous silicon nitride-based ceramic samples did not induce necrotic/apoptotic cell death (cytotoxic effect). However, samples S-5 and S-10 demonstrated cytostatic effects, which was demonstrated by the decrease of cell proliferation.

The results of comet assay used for detection of DNA damage in VH10 and B-HNF-1 cells after 96 h growth with/without the presence of Si₃N₄-SiO₂ samples are shown in **Figure 10**. The results show that no genotoxic effects of Si₃N₄-SiO₂ ceramic discs were observed. The DNA damage values of negative control and Si₃N₄-SiO₂ samples were less than 4.5%. The fluorescence microscopic analysis of the VH10 and B-HNF-1 cells growing with/without the presence of Si₃N₄ samples showed that the control and treated cells had similar morphology and DNA tails (comets) were not observed (**Figure 11**).

4. Conclusions

Porous Si₃N₄-SiO₂-based ceramics with different porosity and pore size were prepared via the free sintering of Si₃N₄ in air with an addition of semolina (5, 10 and 20 wt%) as a pore forming agent. The samples showed a bimodal porosity. The small pores (<5 µm) were created during the controlled sintering of Si₃N₄ powder compact on air at 1360°C and these pores formed a continuous network in the whole volume of the ceramic material. The large pores formed from the added semolina were mostly isolated in ceramic matrix and their size was similar to the pores of bone (~100 µm). The densities of prepared materials were close to those of bones, 1.6 g·cm⁻³ - 2.2 g·cm⁻³. Mercury porosimetry and strength measurements showed that the specific area surface, volume density and compressive strength decreased with the amount of added semolina (amount of large pores). Sam-

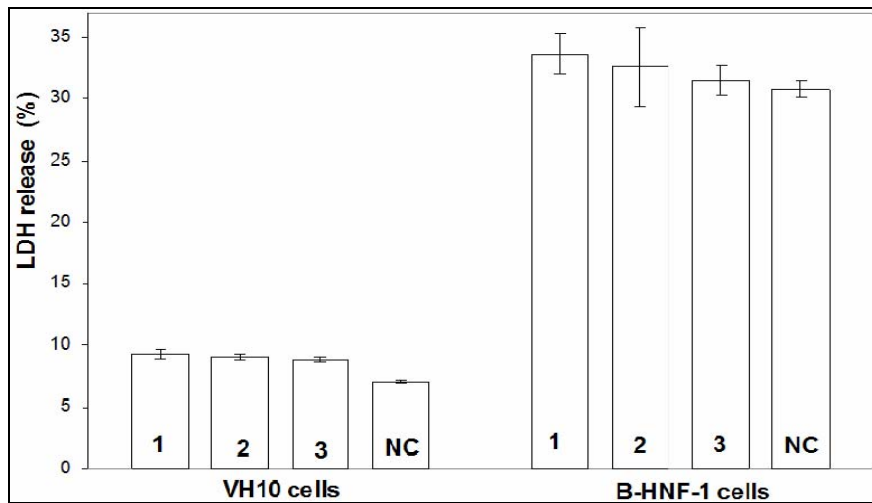


Figure 9. Detected level of lactate dehydrogenase (LDH) release from VH10 and B-HNF-1 cells growing in the presence of S-5 (1), S-10 (2), S-20 (3). The cells growing without the presence of $\text{Si}_3\text{N}_4\text{-SiO}_2$ -based ceramics were used as the negative control (NC).

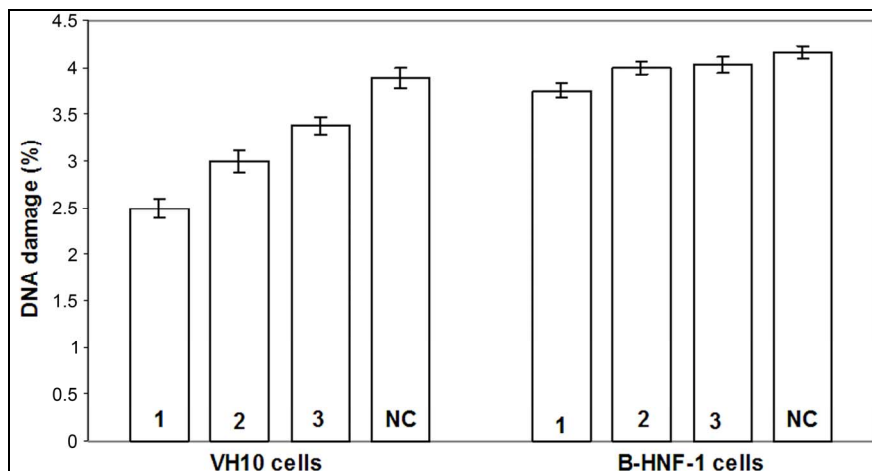


Figure 10. Silicon nitride discs effects on the level of DNA damage in VH10 and B-HNF-1 cells growing 96 h in the presence of samples S-5 (1), S-10 (2), S-20 (3). The cells growing without the presence of $\text{Si}_3\text{N}_4\text{-SiO}_2$ -based ceramic were used as the negative control (NC).

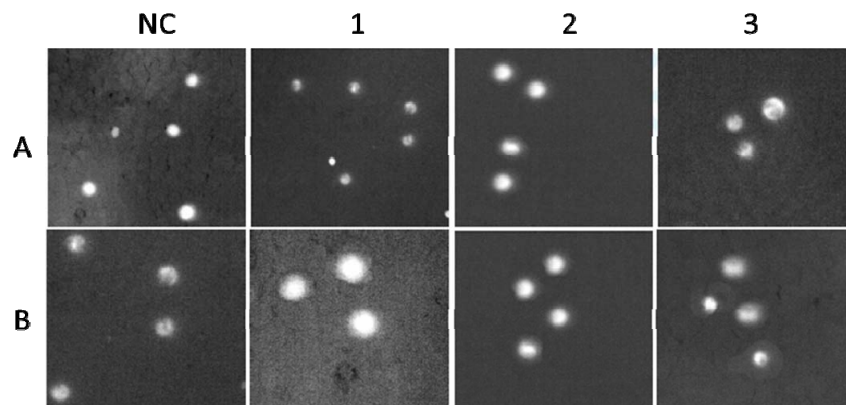


Figure 11. Fluorescence microscopic analysis of DNA damage of VH10 (A) and B-HNF-1 (B) cells growing 96 h in the presence of Si_3N_4 samples S-5 (1), S-10 (2) and S-20 (3). Magnification 400x.

ple containing 20 wt% of semolina has a compressive strength of 370 MPa after sintering which is similar to those of the cortical bone.

Biological tests showed that both tested human fibroblast cell lines (VH10 and B-HNF-1) were sensitive to samples with lower porosity (S-5, S-10). The cell growth inhibition was observed in the range 14.9% - 21.3%. Sample S-20 with the highest porosity (36.4 vol%) had the lowest cytotoxicity (<10%). VH10 and B-HNF-1 cells growing around Si₃N₄-SiO₂-based ceramic discs were homogeneously distributed on the cultivation surface. Significant morphology changes were not found in the treated cells and their morphology was similar to that of the control cells. None of the tested Si₃N₄-SiO₂-based ceramic samples induced necrotic/apoptotic death of human fibroblasts. Comet assay showed that the silicon nitride-based samples did not have genotoxic effects, the control and treated cells had similar morphology and the undesirable DNA tails (comets) were not observed. Among the prepared porous ceramic materials sample S-20 had a similar mechanical properties (compressive strength, density) to bones, very good biocompatibility, slight cytotoxicity and none genotoxicity. Therefore, Si₃N₄-SiO₂-based ceramics prepared by sintering of Si₃N₄ on air with 20 wt% content of semolina as a pore forming additive is a potential material for biomedical applications.

5. Acknowledgements

This study was supported by the Technology Assistance Agency under the contract no. APVV-0500-10 and the Slovak State Committee for Scientific Research VEGA, grant 1/0165/10.

REFERENCES

- [1] B. Cappi, S. Neuss, J. Salber, R. Telle, R. Knüchel and H. Fischer, "Cytocompatibility of High Strength Non-Oxide Ceramics," *Journal of Biomedical Materials Research*, Vol. 93, No. 1, 2009, pp. 67-76.
- [2] F. Bucciotti, M. Mazzocchi and A. Bellosi, "Perspectives of the Si₃N₄-TiN Ceramic Composite as a Biomaterial and Manufacturing of Complex-Shaped Implantable Devices by Electrical Discharge Machining (EDM)," *Journal of Applied Biomaterials and Biomechanics*, Vol. 8, No. 1, 2010, pp. 28-32.
- [3] M. C. Anderson and R. Olsen, "Bone Ingrowth into Porous Silicon Nitride," *Journal of Biomedical Materials Research*, Vol. 92, No. 4, 2010, pp. 1598-1605.
- [4] M. Mazzocchi and A. Bellosi, "On the Possibility of Silicon Nitride as a Ceramic for Structural Orthopaedic Implantans. Part I: Processing, Microstructure, Mechanical Properties, Cytotoxicity," *Journal of Materials Science: Materials in Medicine*, Vol. 19, 2008, pp. 2881-2887.
- [5] M. Mazzocchi, D. Gardini, P. L. Traverso, M. G. Faga and A. Bellosi, "On the Possibility of Silicon Nitride as a Ceramic for Structural Orthopaedic Implantans. Part II: Chemical Stability and Wear Resistance in Body Environment," *Journal of Materials Science: Materials in Medicine*, Vol. 19, 2008, pp. 2889-2901. [doi:10.1007/s10856-008-3417-2](https://doi.org/10.1007/s10856-008-3417-2)
- [6] A. Neumann, M. Kramps, C. Ragoss, H. R. Maier and K. Jahnke, "Histological and Microdiographic Appearances of Silicon Nitride and Aluminium Oxide in a Rabbit Femur Implantation Model," *Materialwissenschaft und Werkstofftechnik*, Vol. 35, No. 9, 2004, pp. 569-573. [doi:10.1002/mawe.200400778](https://doi.org/10.1002/mawe.200400778)
- [7] A. Neumann, K. Jahnke, H. R. Maier and C. Ragoss, "Biocompatibility of Silicon Nitride *in Vitro*. A Comparative Fluorescence-Microscopic and Scanning Electron-Microscopy Study," *Laryngo-Rhino-Otologie*, Vol. 83, 2004, pp. 845-851. [doi:10.1055/s-2004-825739](https://doi.org/10.1055/s-2004-825739)
- [8] A. Neumann, T. Reske, M. Held, C. Ragoss, H. R. Maier and K. Jahnke, "Comparative Investigation of the Biocompatibility of Various Silicon Nitride Ceramic Qualities *in Vitro*," *Journal of Materials Science: Materials in Medicine*, Vol. 15, No. 10, 2004, pp. 1135-1140. [doi:10.1023/B:JMSM.0000046396.14073.92](https://doi.org/10.1023/B:JMSM.0000046396.14073.92)
- [9] R. C. Kue, A. Sohrabi, D. C. Nagle, C. G. Frondoza and D. S. Hungerford, "Enhanced Proliferation and Osteocalcin Production by Human Osteoblast-Like Cells on Silicon Nitride Ceramic Discs," *Biomaterials*, Vol. 20, No. 13, 1999, pp. 1195-1201. [doi:10.1016/S0142-9612\(99\)00007-1](https://doi.org/10.1016/S0142-9612(99)00007-1)
- [10] A. Sohrabi, C. Holland, R. C. Kue, D. Nagle, D. S. Hungerford and C. G. Frondoza, "Proinflammatory Cytokine Expression of IL-1b and TNF-a by Human Osteoblast-Like MG-63 Cells upon Exposure to Silicon Nitride *in Vitro*," *Journal of Biomedical Materials Research*, Vol. 50, 2000, pp. 43-49. [doi:10.1002/\(SICI\)1097-4636\(200004\)50:1<43::AID-JB M7>3.0.CO;2-A](https://doi.org/10.1002/(SICI)1097-4636(200004)50:1<43::AID-JB M7>3.0.CO;2-A)
- [11] C. R. Howlett, E. McCartney and W. Ching, "The Effect of Silicon Nitride Ceramic on Rabbit Skeletal Cell Tissue: An *in Vitro* and *in Vivo* Investigation," *Clinical Orthopaedics and Related Research*, Vol. 244, 1989, pp. 293-304.
- [12] C. C. Guedes e Silva, B. König, M. J. Carbonari, M. Yoshimoto, S. Allegrini and J. C. Bressiani, "Tissue Response around Silicon Nitride Implants in Rabbits," *Journal of Biomedical Materials Research*, Vol. 84A, No. 2, 2008, pp. 337-343. [doi:10.1002/jbm.a.31363](https://doi.org/10.1002/jbm.a.31363)
- [13] C. C. Guedes e Silva, O. Z. Higa and J. C. Bressiani, "Cytotoxic Evaluation of Silicon Nitride Based Ceramics," *Materials Science and Engineering: C*, Vol. 24, No. 5, 2004, pp. 643-646. [doi:10.1016/j.msec.2004.08.007](https://doi.org/10.1016/j.msec.2004.08.007)
- [14] W. Zhang, M. Titze, B. Cappi, D. C. Wirtz and R. Telle, "Improved Mechanical Long-Term Reliability of Hip Resurfacing Prostheses by Using Silicon Nitride," *Journal of Materials Science: Materials in Medicine*, Vol. 21, 2010, pp. 3049-3057. [doi:10.1007/s10856-010-4144-z](https://doi.org/10.1007/s10856-010-4144-z)

- [15] B. S. Bal, R. Lakshminarayanan, A. Khandkar, I. Clarke, A. A. Hoffman and M. N. Rahaman, "In Vitro Performance of Silicon Nitride Ceramic in Total Hip Bearings: Winner of the 2007 'HAP' Paul Award," *Journal of Arthroplasty*, Vol. 24, No. 1, 2009, pp. 110-116. [doi:10.1016/j.arth.2008.01.300](https://doi.org/10.1016/j.arth.2008.01.300)
- [16] J. Gustavsson, G. Altankov, A. Errachid, J. Samitier, J. A. Planell and E. Engel, "Surface Modifications of Silicon Nitride for Cellular Biosensor Applications," *Journal of Materials Science: Materials in Medicine*, Vol. 19, 2008, pp. 1839-1850. [doi:10.1007/s10856-008-3384-7](https://doi.org/10.1007/s10856-008-3384-7)
- [17] G. Kotzar, M. Freas, P. Abel, A. Fleischman, S. Roy, C. Zorman, J. M. Moran and J. Melzak, "Evaluation of MEMS Materials of Construction for Implantable Medical Devices," *Biomaterials*, Vol. 23, No. 13, 2002, pp. 2737-2750. [doi:10.1016/S0142-9612\(02\)00007-8](https://doi.org/10.1016/S0142-9612(02)00007-8)
- [18] G. Voskerician, M. S. Shive, R. S. Shawgo, H. von Recum, J. M. Anderson, M. J. Cima and R. Langer, "Biocompatibility and Biofouling of MEMS Drug Delivery Devices," *Biomaterials*, Vol. 24, No. 11, 2003, pp. 1959-1967. [doi:10.1016/S0142-9612\(02\)00565-3](https://doi.org/10.1016/S0142-9612(02)00565-3)
- [19] S. G. Harris and M. L. Shuler, "Growth of Endothelial Cells on Microfabricated Silicon Nitride Membranes for an *in Vitro* Model of the Blood-Brain Barrier," *Biotechnology and Bioengineering*, Vol. 8, No. 4, 2003, pp. 246-251.
- [20] R. M. Mesquita and A. H. A. Bressiani, "Fabrication of Porous Silicon Nitride by Sacrificing Template Method," *Science and Technology of Advanced Materials*, Vol. 63, 2010, pp. 170-174. [doi:10.4028/www.scientific.net/AST.63.170](https://doi.org/10.4028/www.scientific.net/AST.63.170)
- [21] D. X. Yao, Y.-P. Zeng, K.-H. Zuo and D. L. Jiang, "Porous Si₃N₄ Ceramics Prepared via Nitridation of Si Powder with Si₃N₄ Filler and Postsintering," *International Journal of Applied Ceramic Technology*, Vol. 1, No. 1, 2011, pp. 1-7.
- [22] J. Xu, D. Zhu, F. Luo, W. Zhou and P. Li, "Dielectric Properties of Porous Reaction-Boned Si₃N₄ Ceramics with Controlled Porosity and Pore Size," *Journal of Materials Science and Technology*, Vol. 24, No. 2, 2008, pp. 207-210.
- [23] C. R. Rambo, H. Sieber and L. A. Genova, "Synthesis of Porous Biomorphic α/β -Si₃N₄ Composite from Sea Sponge," *Journal of Porous Materials*, Vol. 15, No. 4, 2008, pp. 419-425. [doi:10.1007/s10934-007-9101-y](https://doi.org/10.1007/s10934-007-9101-y)
- [24] A. Díaz and S. Hampshire, "Characterisation of Porous Silicon Nitride Materials Produced with Starch," *Journal of the European Ceramic Society*, Vol. 24, No. 2, 2004, pp. 413-419. [doi:10.1016/S0955-2219\(03\)00212-7](https://doi.org/10.1016/S0955-2219(03)00212-7)
- [25] S. Ding, Z. P. Zeng and D. Jiang, "Oxidation Bonding of Porous Silicon Nitride Ceramics with High Strength and Low Dielectric Constant," *Materials Letters*, Vol. 61, No. 11-12, 2007, pp. 2277-2280. [doi:10.1016/j.matlet.2006.08.067](https://doi.org/10.1016/j.matlet.2006.08.067)
- [26] B. T. Lee and H. D. Kim, "Effect of Sintering Additives on the Nitridation Behaviour of Reaction Bonded Silicon Nitride," *Materials Science and Engineering*, Vol. A364, 2004, pp. 126-131.
- [27] F. L. Yu, H. R. Wang, Y. Bai and J. F. Yang, "Preparation and Characterization of Porous Si₃N₄ Ceramics Prepared by Compression Molding and Slip Casting Methods," *Bulletin of Materials Science*, Vol. 33, No. 5, 2010, pp. 619-624. [doi:10.1007/s12034-010-0094-9](https://doi.org/10.1007/s12034-010-0094-9)
- [28] J. F. Yang, Z. Y. Deng and T. Ohji, "Fabrication and Characterization of Porous Silicon Nitride Ceramics Using Yb₂O₃ as Sintering Additive," *Journal of the European Ceramic Society*, Vol. 23, No. 2, 2003, pp. 371-378. [doi:10.1016/S0955-2219\(02\)00175-9](https://doi.org/10.1016/S0955-2219(02)00175-9)
- [29] F. Chen, Q. Shen, F. Yan and L. Zhang, "Pressureless Sintering of α -Si₃N₄ Porous Ceramics Using a H₃PO₄ Pore-Forming Agent," *Journal of the American Ceramic Society*, Vol. 90, No. 8, 2007, pp. 2379-2383. [doi:10.1111/j.1551-2916.2007.01800.x](https://doi.org/10.1111/j.1551-2916.2007.01800.x)
- [30] M. Theisova, S. Jantová, S. Letašiová, L. Valík and M. Palou, "Comparative Study of a New Composite Biomaterial Fluor-Hydroxyapatite on Fibroblast Cell Line NIH-3T3 by Direct Test," *Biologia*, Vol. 63, No. 2, 2008, pp. 273-281. [doi:10.2478/s11756-008-0043-x](https://doi.org/10.2478/s11756-008-0043-x)
- [31] H. U. Bergmeier, "Methoden der Enzymatischen Analyse," 2nd Edition, Akademie Verlag, Berlin, 1970.
- [32] S. Jantová, M. Theiszová, P. Matejov and D. Bakoš, "Biocompatibility and Cytotoxicity of Bioglass-Ceramic Composite with Various P₂O₅ Content in Li₂O-SiO₂-CaO-CaF₂-P₂O₅ System on Fibroblast Cell Lines," *Acta Chimica Slovaca*, Vol. 4, No. 1, 2011, pp. 15-30.
- [33] V. J. McKelvey-Martin, M. H. Green, P. Schmezer, B. L. Pool-Zobel, M. P. De Méo and A. R. Collins, "The Single Cell Gel Electrophoresis Assay (Comet Assay): A European Review," *Mutation Research*, Vol. 288, No. 1, 1993, pp. 47-63. [doi:10.1016/0027-5107\(93\)90207-V](https://doi.org/10.1016/0027-5107(93)90207-V)
- [34] N. P. Singh, M. T. McCoy, R. R. Tice and E. L. Schneider, "A Simple Technique for Quantitation of Low Levels of DNA Damage in Individual Cells," *Experimental Cell Research*, Vol. 175, 1988, pp. 84-91. [doi:10.1016/0014-4827\(88\)90265-0](https://doi.org/10.1016/0014-4827(88)90265-0)
- [35] D. Slameňova, A. Gabelova, L. Ruzekova, I. Chalupa, E. Horvathova, T. Farkasova, E. Bozsakyova and R. Stetina, "Detection of MNNG-Induced DNA Lesions in Mammalian Cells; Validation of Comet Assay against DNA Unwinding Technique, Alkaline Elution of DNA and Chromosomal Aberrations," *Mutation Research*, Vol. 383, 1997, pp. 243-252. [doi:10.1016/S0921-8777\(97\)00007-4](https://doi.org/10.1016/S0921-8777(97)00007-4)
- [36] A. Gabelova, D. Slameňova, L. Ruzekova, T. Farkasova and E. Horvathova, "Measurement of DNA Strand Breakage and DNA Repair Induced with Hydrogen Peroxide Using Single Cell Gel Electrophoresis, Alkaline DNA Unwinding and Alkaline Elution of DNA," *Neoplasma*, Vol. 44, No. 6, 1997, pp. 380-388.
- [37] A. R. Collins, A. G. Ma and S. J. Duthie, "The Kinetics of Repair of Oxidative DNA Damage (Strand Breaks and Oxidised Pyrimidines) in Human Cells," *Mutation Research/DNA Repair*, Vol. 336, No. 1, 1995, pp. 69-77. [doi:10.1016/0921-8777\(94\)00043-6](https://doi.org/10.1016/0921-8777(94)00043-6)
- [38] S. Wada, "Control of Instability of Si₃N₄ during Pres-

- sureless Sintering,” *Journal of the Ceramic Society of Japan*, Vol. 109, No. 1247, 2001, pp. 803-808.
[doi:10.2109/jcersj.109.1274_803](https://doi.org/10.2109/jcersj.109.1274_803)
- [39] G. D. Sorarù, S. Modena, E. Guadagnino, P. Colombo, J. Egan and C. Pantano, “Chemical Durability of Oxycarbide Glasses,” *Journal of the American Ceramic Society*, Vol. 85, No. 6, 2002, pp. 1529-1536.
[doi:10.1111/j.1151-2916.2002.tb00308.x](https://doi.org/10.1111/j.1151-2916.2002.tb00308.x)
- [40] M. Amaral, M. A. Lopes, R. F. Silva and J. D. Santos, “Densification Route and Mechanical Properties of Si₃N₄-Bioglass Biocomposites,” *Biomaterials*, Vol. 23, No. 3, 2002, pp. 857-862. [doi:10.1016/S0142-9612\(01\)00194-6](https://doi.org/10.1016/S0142-9612(01)00194-6)
- [41] M. Amaral, M. A. Costa, M. A. Lopes, R. F. Silva, J. D. Santos and M. H. Fernandes, “Si₃N₄-Bioglass Composites Stimulate the Proliferation of MG63 Osteoblast-Like Cells and Support the Osteogenic Differentiation of Human Bone Marrow Cells,” *Biomaterials*, Vol. 23, No. 24, 2002, pp. 4897-4906.
[doi:10.1016/S0142-9612\(02\)00249-1](https://doi.org/10.1016/S0142-9612(02)00249-1)
- [42] M. F. Morks, “Fabrication and Characterization of Plasma-Sprayed HA/SiO₂ Coatings for Biomedical Application,” *Journal of the Mechanical Behavior of Biomedical Materials*, Vol. 1, No. 1, 2008, pp. 105-111.
[doi:10.1016/j.jmbbm.2007.04.003](https://doi.org/10.1016/j.jmbbm.2007.04.003)
- [43] A. Diaz, T. Lopez, J. Manjarrez, E. Basadella, J. M. Martinez-Blanes and J. A. Odriozola, “Growth of Hydroxyapatite in a Biocompatible Mesoporous Ordered Silica,” *Acta Biomaterialia*, Vol. 2, No. 2, 2006, pp. 173-179.
[doi:10.1016/j.actbio.2005.12.006](https://doi.org/10.1016/j.actbio.2005.12.006)
- [44] Y. Xie, X. Zheng, C. Ding, X. Liu and P. K. Chu, “Mechanism of Apatite Formation on Silicon Suboxide Film Prepared by Pulsed Metal Vacuum Arc Deposition,” *Materials Chemistry and Physics*, Vol. 109, No. 2-3, 2008, pp. 342-346.
[doi:10.1016/j.matchemphys.2007.11.039](https://doi.org/10.1016/j.matchemphys.2007.11.039)
- [45] S. Zhang, L. Xia, C. H. Kang, G. Xiao, S. M. Ong, Y. C. Toh, H. L. Leo, D. van Noort, S. H. Kan, H. H. Tang and H. Yu, “Microfabricated Silicon Nitride Membranes for Hepatocyte Sandwich Culture,” *Biomaterials*, Vol. 29, No. 29, 2008, pp. 3993-4002.
[doi:10.1016/j.biomaterials.2008.06.024](https://doi.org/10.1016/j.biomaterials.2008.06.024)
- [46] A. J. Dulgar-Tulloch, R. Biyios and R. W. Siegel, “Human Mesenchymal Stem Cell Adhesion and Proliferation in Response to Ceramic Chemistry and Nanoscale Topography,” *Journal of Biomedical Materials Research Part A*, Vol. 90A, No. 2, 2009, pp. 586-594.
[doi:10.1002/jbm.a.32116](https://doi.org/10.1002/jbm.a.32116)
- [47] J. Gustavsson, G. Altankov, A. Errachid, J. Samitier, J. A. Planell and E. Engel, “Surface Modifications of Silicon Nitride for Cellular Biosensor Applications,” *Journal of Materials Science: Materials in Medicine*, Vol. 19, No. 4, 2008, pp. 1839-1850. [doi:10.1007/s10856-008-3384-7](https://doi.org/10.1007/s10856-008-3384-7)
- [48] E. A. Carter, B. S. Rayner, A. I. McLeod, L. E. Wu, C. P. Marshall, A. Levina, J. B. Aitken, P. K. Witting, B. Lai, Z. Cai, S. Vogt, Y. C. Lee, C. I. Chen, M. J. Tobin, H. H. Harris and P. A. Lay, “Silicon Nitride as a Versatile Growth Substrate for Microspectroscopic Imaging and Mapping of Individual Cells,” *Molecular BioSystems*, Vol. 6, No. 7, 2010, pp. 1316-1322. [doi:10.1039/c001499k](https://doi.org/10.1039/c001499k)
- [49] I. Svensson, E. Artursson, P. Leanderson, R. Berglind and F. Lindgren, “Toxicity *in Vitro* of Some Silicon Carbides and Silicon Nitrides: Whiskers and Powders,” *American Journal of Industrial Medicine*, Vol. 31, No. 3, 1997, pp. 335-343.
[doi:10.1002/\(SICI\)1097-0274\(199703\)31:3<335::AID-AJIM10>3.0.CO;2-1](https://doi.org/10.1002/(SICI)1097-0274(199703)31:3<335::AID-AJIM10>3.0.CO;2-1)
- [50] G. L. Fisher, K. L. McNeill and J. T. Smith, “*In Vitro* Effects of Fibrous and Nonfibrous Silicon Nitride on Bovine Pulmonary Macrophages,” *Environmental Research*, Vol. 50, No. 2, 1989, pp. 279-288.